PHYSICAL REVIEW B **79**, 214410 (2009)

Exotic magnetism in the alkali sesquioxides Rb_4O_6 and Cs_4O_6

Jürgen Winterlik, Gerhard H. Fecher, Catherine A. Jenkins, Sergey Medvedev, and Claudia Felser*
Institute for Inorganic and Analytic Chemistry, Johannes Gutenberg-Universität, D-55099 Mainz, Germany

Jürgen Kübler
Institute for Solid State Physics, Technische Universität, 64289 Darmstadt, Germany

Claus Mühle, Klaus Doll, and Martin Jansen†
Max-Planck-Institute for Solid State Research, 70569 Stuttgart, Germany

Taras Palasyuk, Ivan Trojan, and Mikhail I. Eremets
Max-Planck-Institute for Chemistry, 55020 Mainz, Germany

Franziska Emmerling
Bundesanstalt Materialforschung und Prüfung Berlin, 12489 Berlin, Germany
(Received 20 February 2009; revised manuscript received 28 April 2009; published 9 June 2009)

Among the various alkali oxides the sesquioxides Rb_4O_6 and Cs_4O_6 are of special interest. Electronic-structure calculations using the local spin-density approximation predicted that Rb_4O_6 should be a half-metallic ferromagnet, which was later contradicted when an experimental investigation of the temperature-dependent magnetization of Rb_4O_6 showed a low-temperature magnetic transition and differences between zero-field-cooled and field-cooled measurements. Such behavior is known from spin glasses and frustrated systems. Rb_4O_6 and Cs_4O_6 comprise of two different types of dioxygen anions, the hyperoxide and the peroxide anions. The nonmagnetic peroxide anions do not contain unpaired electrons while the hyperoxide anions contain unpaired electrons in antibonding π^* orbitals. High electron localization (narrow bands) suggests that electronic correlations are of major importance in these open-shell *p*-electron systems. Correlations and charge ordering due to the mixed valency render *p*-electron-based anionogenic magnetic order possible in the sesquioxides. In this work we present an experimental comparison of Rb_4O_6 and the related Cs_4O_6. The crystal structures are verified using powder x-ray diffraction. The mixed valency of both compounds is confirmed using Raman spectroscopy, and time-dependent magnetization experiments indicate that both compounds show magnetic frustration, a feature only previously known from *d*- and *f*-electron systems.

DOI: 10.1103/PhysRevB.79.214410 PACS number(s): 75.50.−y, 71.20.Be, 68.47.Gh

I. INTRODUCTION

Magnetism arising from *d* and *f* shells has drawn the bulk of research attention but *p*-electron-based magnetic order is a rare and fascinating topic that presents the added challenge of molecular and not just atomic ordering. The majority of main group molecules are nonmagnetic. Few exceptions are found, e.g., in NO, NO_2, and O_2. Molecular oxygen contains two single electrons in degenerate antibonding π^* orbitals, which can order magnetically in a solid crystal. Solid oxygen shows a large variety of magnetic phenomena ranging from antiferromagnetism to superconductivity.[1–5]

What applies to molecular oxygen applies equally to charged oxygen molecules with unpaired electrons. Dioxygen anions are principally found in alkali and alkaline-earth oxides, which represent excellent model systems because of their supposedly simple electron configurations. The hyperoxide anion O_2^- corresponds to "charged oxygen." Since it still contains one unpaired electron, magnetic order is enabled for hyperoxides. KO_2, RbO_2, and CsO_2 are known to exhibit antiferromagnetic ordering below their respective Néel temperatures of 7, 15, and 9.6 K, respectively.[6,7]

Among the alkali oxides, the sesquioxides are of special interest. In contrast to related compounds, which are white, yellow, or orange, the sesquioxides Rb_4O_6 and Cs_4O_6 are black. Furthermore, a formula unit AM_4O_6 (AM=alkali metals Rb or Cs) contains two different types of dioxygen anions: one closed-shell nonmagnetic peroxide anion and two of the aforementioned hyperoxide anions. The structural formula of the sesquioxides is thus accurately represented as $(AM^+)_4(O_2^-)_2(O_2^{2-})$.[8] The mixed valency enables complicated magnetic structures in the sesquioxides. The first descriptions of the crystal structures of the sesquioxides were published in 1939 in the pioneering works of Helms and Klemm.[9–11] Both compounds belong to the Pu_2C_3 structure type and to space group $I\bar{4}3d$. This Pu_2C_3 structure type is known from the noncentrosymmetric rare-earth metal sesquicarbide superconductors such as Y_2C_3 with a maximum critical temperature of T_c=18 K.[12] For Cs_4O_6, the literature runs out after 1939 because of the extremely challenging synthesis and sensitivity to air. In Rb_4O_6, the presence of both peroxide and hyperoxide anions was verified by neutron-scattering,[13] and electronic-structure calculations using the local spin-density approximation were performed to explain the exceptional black color.[14] These same calculations predicted a half-metalllic ferromagnetic ground state but were contradicted by later experiments in which a transition was found to occur at approximately 3.4 K in the

temperature-dependent magnetization.[15] Differences between zero-field-cooled (ZFC) and field-cooled (FC) measurements indicated that Rb_4O_6 behaves like a frustrated system or a spin glass. Recently published electronic-structure calculations are consistent with the experimental findings.[16] It was shown that for an accurate theoretical treatment of highly localized systems such as Rb_4O_6 and Cs_4O_6, a symmetry reduction, exact exchange, and electron-electron correlations have to be considered in the calculations. This can be generalized to any other open-shell system that is based on *p* electrons. Accounting for these features the calculations result in an insulating ground state. Further calculations using the spin spiral method show that Rb_4O_6 exhibits spin spiral behavior in a certain crystal direction. The energy changes are extremely small along this direction indicating a multidegenerate ground state.[16] In this work we present the routes of synthesis for Rb_4O_6 and Cs_4O_6 and the structural verification using powder x-ray diffraction (XRD). Raman spectroscopic measurements confirm the mixed valency of the used Rb_4O_6 and Cs_4O_6 samples. Magnetization experiments are shown that indicate a dynamic time-dependent magnetism of Rb_4O_6. Furthermore we present a comprehensive experimental study of Cs_4O_6, which has not been extensively investigated due to the difficulty of sample preparation. Magnetization measurements dependent on temperature, magnetic field, and time provide evidence that Cs_4O_6 shows a similar behavior as Rb_4O_6. According to experimental and theoretical investigations,[16] both sesquioxides are mixed valent highly correlated systems exhibiting *p*-electron-based magnetic frustration. These seemingly simple compounds can serve as model systems for any other open-shell systems that are based on *p* electrons such as hole-doped MgO (Ref. 17) or nanographene.[18]

II. STRUCTURE

Figure 1 depicts a body-centered-cubic unit cell of AM_4O_6. The 24 oxygen atoms in the cubic cell form 12 molecules that can be distinguished both by their valency and by their alignment along the principal axes. We assumed the nonmagnetic peroxide anions to be oriented along the *z* axis, whereas the hyperoxides are oriented along the *x* and *y* axes. The experimental bond lengths for the hyperoxide and the peroxide anions are $0.144a$ and $0.165a$, respectively.[19,20] The cubic lattice parameters are found in Sec. IV.

III. SYNTHESIS

The precursors rubidium and cesium oxide AM_2O as well as rubidium and cesium hyperoxide AMO_2 were prepared from elemental sources. For AM_2O, liquid rubidium/cesium, purified by distillation, was reacted with a stoichiometric amount of dry oxygen in an evacuated glass tube followed by heating at 473 K for 2 weeks under argon atmosphere.[21,22] The samples were subsequently ground under argon and the entire cycle was repeated five times. A slight excess of rubidium/cesium was distilled at 573 K in vacuum, resulting in a pale green powder of Rb_2O and an orange powder of Cs_2O. AMO_2 were prepared through the reaction of liquid rubidium/cesium and an excess of dry oxygen using the same method as described for AM_2O, resulting in yellow powders of RbO_2 and CsO_2, respectively.

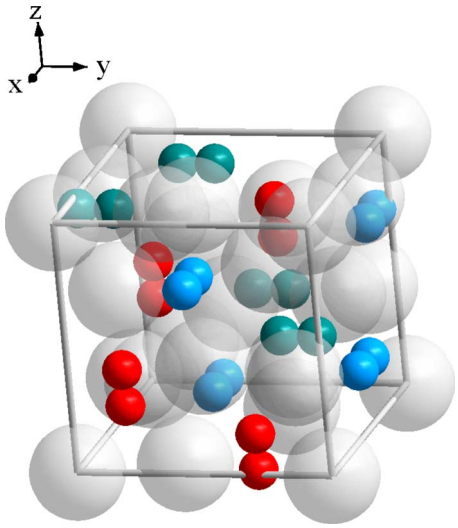

FIG. 1. (Color online) Pseudobody-centered-cubic cell of the alkali sesquioxides AM_4O_6 (AM=Rb, Cs). Differently oriented dioxygen anions are drawn with different colors so that the alignment along the axes can be distinguished. For clarity, the Rb/Cs atoms are gray and transparent.

Rb_4O_6 was obtained by a solid-state reaction of 400 mg RbO_2 and 160 mg Rb_2O in a molecular ratio of 4:1 in a glass tube sealed under argon at 453 K for 24 h. Cs_4O_6 was obtained in the same way using the amounts of 468 mg CsO_2 and 280 mg Cs_2O and annealing at 473 K for 24 h. For the reaction, a slight excess of Cs_2O was used to compensate for small amounts of cesium peroxide, which is always contained as an impurity in Cs_2O. The very air-sensitive products were ground and the reaction was repeated until pure phases were obtained (black powders). For the magnetization measurements, Rb_4O_6 and Cs_4O_6 were sealed in a high-purity quartz tube (Suprasil® glass) under helium atmosphere.

IV. STRUCTURAL CHARACTERIZATION

The crystal structures of the compounds were investigated using XRD. The measurements were carried out using a Bruker D8 diffractometer with Cu $K\alpha 1$ radiation for Rb_4O_6 and Mo $K\alpha 1$ for Cs_4O_6. The samples were measured in sealed capillary tubes under an argon atmosphere. The diffraction patterns are shown in Fig. 2. The raw data (black) are compared to the difference between a calculated Rietveld refinement and the raw data (gray). The refinements yielded weighted profile *R* values of $R_{wp}=8.216$ for Rb_4O_6 and 6.388 for Cs_4O_6. Both compounds crystallize in the cubic structure $I\bar{4}3d$ (space group 220). The experimental lattice parameters as found from Rietveld refinements are 9.322 649(74) Å for Rb_4O_6 and 9.845 83(11) Å for Cs_4O_6. The atomic parameters for both compounds are shown in Table I and additional structural information is found in Table II. The pattern of Rb_4O_6 indicates good phase purity. In the case of Cs_4O_6,

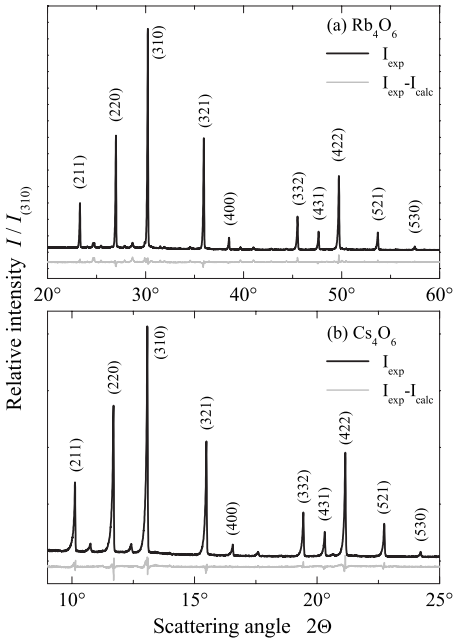

FIG. 2. Powder x-ray diffraction patterns of Rb_4O_6 and Cs_4O_6 at 300 K (black). The gray curves show the differences between the observed data and the Rietveld refinements.

additional signals were detected. The signals were identified to arise from the impurity CsO_2, which belongs to the cubic space group $Fm\bar{3}m$ and has a lattice parameter of a =6.552 96(37) Å. The impurity phase was included in the refinement of Cs_4O_6. An impurity content of approximately 7.23% of CsO_2 in Cs_4O_6 was derived from the refinement.

V. RAMAN SPECTROSCOPY

The presence of peroxide and hyperoxide anions in Rb_4O_6 and Cs_4O_6 was verified using Raman spectroscopy. The measurements were performed using a diamond-anvil cell in order to prevent sample decomposition from contact with air and moisture. The samples were loaded in a dry box under dry nitrogen atmosphere. The samples were confined within a cylindrical hole of 100 μm diameter and 50 μm height drilled in a Re gasket. We used synthetic type-IIa diamond anvils, which have only traces of impurities (<1 ppm) and very low intrinsic luminescence. Raman spectra were recorded with a single 460-mm-focal-length imaging spectrometer (Jobin Yvon HR 460) equipped with 900 and 150 grooves/mm gratings, giving a resolution of 15 cm^{-1}, notch-filter (Kaiser Optics), liquid nitrogen cooled charge-coupled device (Roper Scientific). Scattering calibration was done using Ne lines with an uncertainty of ± 1 cm^{-1}. The He-Ne laser of Melles Griot with the wavelength of 632.817 nm was used for excitation of the sample. The probing area was a spot with 5 μm diameter. Figure 3 shows the Raman spectrum of Rb_4O_6 in a range from 700–1250 cm^{-1}. Two peaks are found at Raman shifts of 795 and 1153 cm^{-1}, respectively. The signal at 795 cm^{-1} corresponds to the stretching vibration of the peroxide anions and is in good agreement with the literature value of 782 cm^{-1} for Rb_2O_2.[23] The peak at 1153 cm^{-1} is assigned to the corresponding vibration of the hyperoxide anions and comparable to the literature value of 1140 cm^{-1} for RbO_2.[24] In the Raman spectrum for Cs_4O_6, which was recorded as described above, signals of 738 and 1128 cm^{-1} were recorded. The simultaneous presence of both dioxygen anion types and thus the mixed valency is proven for both Rb_4O_6 and Cs_4O_6.

TABLE I. Atomic parameters for Rb_4O_6 and Cs_4O_6. (a) In the cubic space group $I\bar{4}3d$ (No. 220) all alkali or oxygen atoms are equivalent. $q=d/(2a)$ is the relative position parameter of the oxygen atoms that depends on the bond length d of the dioxygen anions and the lattice parameter a. (b) In space group $I2_12_12_1$ (No. 24) each pair O^{ij} ($i=1,2,3$, $j=1,2$) forms one set of O_2 anions. The centers of these anions are located at (7/8, 0, 1/4), (1/4, 7/8, 0), and (0, 1/4, 7/8). q_1 and q_2 (for values see Table II) are the relative position parameters of the peroxide and hyperoxide anions, respectively. All permutations of q_1 and q_2 lead to the same structure.

Atom	Site	x	y	z
		$I\bar{4}3d$		
AM	16c	t	t	t
O	24d	$3/8-q$	0	3/4
Rb	16c	1.054696(50)	1.054696(50)	1.054696(50)
O	24d	1.20206(36)	0	3/4
Cs	16c	0.946544(45)	0.946544(45)	0.946544(45)
O	24d	0.55065(49)	0	3/4
		$I2_12_12_1$		
AM^1	8d	$1/4-t$	$1/4-t$	$1/4-t$
AM^2	8d	$1/2-t$	$1/2-t$	$1/2-t$
O^{11}	4a	$7/8-q_2$	0	1/4
O^{12}	4a	$7/8+q_2$	0	1/4
O^{21}	4b	1/4	$7/8-q_2$	0
O^{22}	4b	1/4	$7/8+q_2$	0
O^{31}	4c	0	1/4	$7/8-q_1$
O^{32}	4c	0	1/4	$7/8+q_1$

VI. MAGNETIZATION

The magnetic properties of Rb_4O_6 and Cs_4O_6 were investigated using a superconducting quantum interference device (Quantum Design MPMS-XL5). Samples of approximately 100 mg, fused in Suprasil tubes under helium atmosphere, were used for the analysis. In the cases of temperature-dependent and time-dependent magnetometry we performed under ZFC and FC measurements. For the ZFC conditions, the samples were first cooled to a temperature of 1.8 K without applying a magnetic field. After applying an induction field $\mu_0 H$, the magnetization was recorded as a function of temperature or time. For the temperature-dependent measurements, the magnetization was recorded directly afterward in the same field upon lowering the temperature down to 1.8 K again (FC).

Temperature-dependent magnetization experiments were discussed in an earlier work[15] and indicate that Rb_4O_6 be-

TABLE II. Structural parameters for the alkali sesquioxides AM_4O_6. Cs data from Ref. 11; Rb data from Refs. 8 and 13 for powder XRD (pd), single-crystal (sc) XRD, and powder neutron diffraction (nd). $q=d/(2a)$ is the mean parameter from XRD measurements; q_2 and q_1 are the parameters calculated for O_2^- and O_2^{--} ions, respectively (see text).

AM	a (Å)	t	d (Å)	q	q_2	q_1	Method
Rb	9.3242	0.0545	1.3426	0.072			pd
Rb (295 K)	9.3327	0.05411	1.3234	0.0709			sc
Rb (213 K)	9.2884	0.05377	1.3115	0.0706	0.0721	0.0829	sc
Rb (5 K)	9.2274	0.05395	1.363	0.0738	0.0726	0.0834	nd
Cs	9.86	0.054			0.068	0.078	pd

haves like a frustrated system. We have analyzed the related Cs_4O_6 using an identical experimental setup. Figures 4(a) and 4(b) display the temperature-dependent magnetization of Cs_4O_6 at magnetic induction fields $\mu_0 H$ of 2 mT and 5 T, respectively. The measurements were carried out under ZFC conditions and FC conditions. In the 2 mT ZFC measurement, a magnetic transition is found to occur at 3.2 ± 0.2 K. In the 5 T ZFC curve, this transition shows a distinct broadening and is shifted to a higher temperature. Thermal irreversibilities between ZFC and FC measurements are observed in both magnetic fields, a behavior known from frustrated systems and spin glasses. Cs_4O_6 exhibits similar magnetic properties as Rb_4O_6.

Figure 5 shows Curie-Weiss fits of Rb_4O_6 and Cs_4O_6 in temperature ranges of 100–300 K at magnetic fields of 5 T. The fits were performed in the region above 200 K and yield negative paramagnetic transition temperatures for both compounds [$\Theta_D=-6.9$ K for Rb_4O_6 (Ref. 15) and $\Theta_D=-4.5$ K for Cs_4O_6]. This indicates dominance of antiferromagnetic interactions. From the high-temperature data, an effective magnetic moment of $m=1.83\mu_B$ per hyperoxide anion can be deduced applying the Curie-Weiss law based on molecular-field theory (MFT) for Rb_4O_6, whereas the moment was calculated to amount to $m=2.01\mu_B$ for Cs_4O_6. These values are in modest agreement with $1.73\mu_B$ as expected from MFT using the spin-only approximation. The inverse susceptibility of Cs_4O_6 exhibits a broad peak at approximately 210 K. The origin of this peak is not clear. Several alkali oxides are, however, known to show multiple phase transitions,[7,25] which are in some cases even very small changes in the lattice parameters. The peak may correspond to such a phase transition.

We also performed field-dependent magnetization measurements. Figure 6(a) shows the field-dependent magnetization of Rb_4O_6 at 2 K, well below the magnetic transition temperature of 3.4 K. It is clear that the magnetization does not show hysteresis [see inset (i)]. The shape of the magnetization curve is best modeled by a paramagnetic loop correction to a Langevin function $L(H)$ given by $M(H)=\chi_{lin}H+M_0L(H)$, where χ_{lin} is the field-independent paramagnetic susceptibility and M_0 is the saturation moment. In inset (ii), the linear contribution was subtracted from the total magnetization. The remaining Langevin function saturates initially with a magnetic moment of $0.25\mu_B/Rb_4O_6$ f.u. and increases in successive cycles. At given magnetic fields, the up

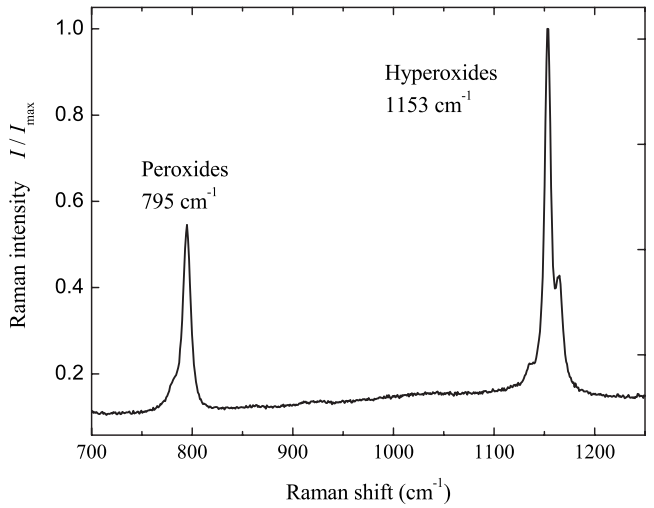

FIG. 3. Raman spectrum of Rb_4O_6. The peak at 795 cm^{-1} corresponds to the stretching vibration of the peroxide anions and the peak at 1153 cm^{-1} corresponds to the stretching vibration of the hyperoxide anions.

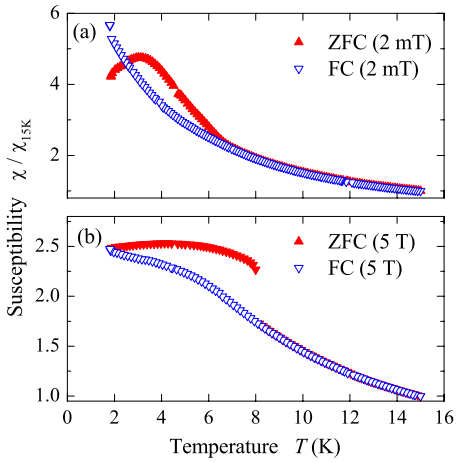

FIG. 4. (Color online) Shown is the temperature-dependent magnetic susceptibility of Cs_4O_6. The low-temperature behavior is shown in (a) and (b) for induction fields of 2 mT and 5 T, respectively. (All values are normalized by the value of the susceptibility at 2 K.)

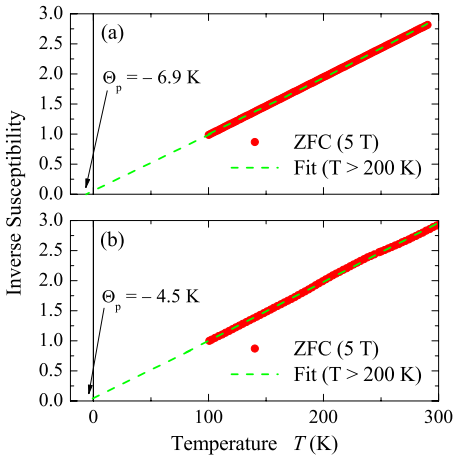

FIG. 5. (Color online) Curie-Weiss fits of Rb_4O_6 (Ref. 15) and Cs_4O_6. The data of Rb_4O_6 are shown in (a) and the data of Cs_4O_6 are shown in (b). The dashed lines represent a Curie-Weiss fit in the temperature region above 200 K. (All values are normalized by the values of the inverse susceptibilities at 100 K.)

and down curves exhibit differences in the measured magnetization, indicating that the magnetization changes with time in a manner consistent with the known relaxation behavior of frustrated systems.[26] Figure 6(b) shows the corresponding field-dependent magnetization for Cs_4O_6, qualitatively similar to Rb_4O_6. Applying the model of the paramagnetic loop correction to a Langevin function as described above a saturation magnetic moment of $0.37\mu_B/Cs_4O_6$ f.u. is obtained as seen in Fig. 6(b), inset (ii). While the total magnetic moments of Rb_4O_6 and Cs_4O_6 are quite similar at given magnetic fields, the paramagnetic contributions exhibit a large

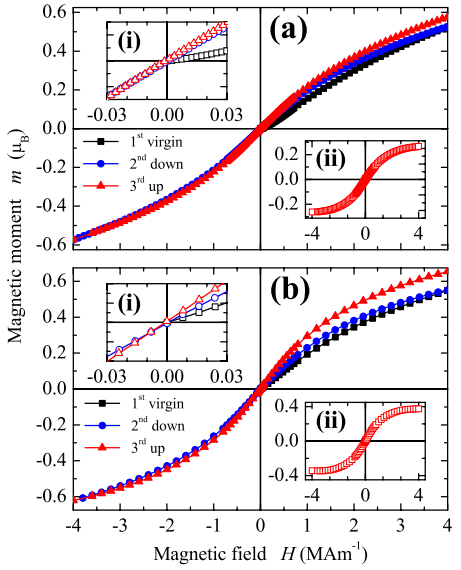

FIG. 6. (Color online) Field-dependent magnetization of Rb_4O_6 and Cs_4O_6 at $T=2$ K. Shown are three magnetization cycles as a function of applied H: virgin ($0 \rightarrow +H_{max}$), down ($+H_{max} \rightarrow -H_{max}$), and up ($-H_{max} \rightarrow +H_{max}$). The insets (i) show in detail the magnetization close to the origin. The insets (ii) show the remaining Langevin functions after subtracting the linear paramagnetic correction.

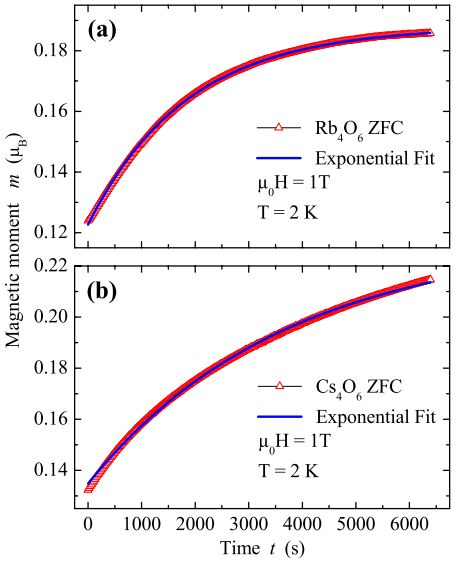

FIG. 7. (Color online) Time-dependent magnetizations of Rb_4O_6 and Cs_4O_6 in induction fields of $\mu_0 H=1$ T are shown. The solid lines are the result of exponential fits.

difference. This indicates that the time dependence and the dynamics of the compounds are differing.

Time-dependent measurements reveal more about these dynamics. Figures 7(a) and 7(b) show the time-dependent variations in the magnetization up to 6400 s for both compounds. The measurements were performed under ZFC conditions at 2 K in induction fields of 1 T. The magnetic moment of Rb_4O_6 varies exponentially with a relaxation time of $\tau=1852\pm30$ s. This value is comparable to those of other frustrated systems. Similar curves were obtained for Rb_4O_6 using lower as well as higher induction fields of 30 mT and 5 T. The relaxation times were determined to be $\tau(30\ \text{mT})=1170\pm30$ s and $\tau(5\ \text{T})=4340\pm20$ s. The pronounced relaxation is another clear indication of the magnetic frustration in Rb_4O_6.

As in the case of Rb_4O_6, the magnetic moment of Cs_4O_6 follows exponential behavior. A relaxation time of $\tau=3701\pm30$ s is deduced from the exponential fit confirming that Cs_4O_6 is also a magnetically frustrated $2p$ system although with different dynamics. The fitting curve does not follow the exponential behavior as exactly as for Rb_4O_6. This is most probably due to the fact that a complete saturation of the magnetization is not reached within the time span of 6400 s. A reason for these differences between the compounds cannot be given within the scope of these experiments, but electronic-structure calculations for Cs_4O_6 may shed more light on the dynamics of this system.

VII. SUMMARY AND CONCLUSIONS

It has been shown that the alkali sesquioxides Rb_4O_6 and Cs_4O_6 exhibit frustrated magnetic ordering based on anionogenic $2p$ electrons of the hyperoxide anions. Mixed valency was verified in both compounds using Raman spectroscopy. The strong time dependence of the magnetization and the pronounced differences between the ZFC and FC measure-

ments support the previously assumed frustrated state of Rb_4O_6.[16] Cs_4O_6 was found to show a very similar behavior. The experiments show that strong electronic correlations can also occur in presumably simple $2p$ compounds such as alkali oxides. The complex distribution of magnetic moments in the lattices leads to a symmetry reduction and causes a frustrated magnetic behavior in both compounds. These results are of major importance since they confirm that open-shell p electrons can behave like d or f electrons.

This work was funded by the DFG in the Collaborative Research Center, *Condensed Matter Systems with Variable Many-Body Interactions*, under Grant No. TRR 49. The authors are grateful for the fruitful discussions with W. Pickett, M. Jourdan, G. Jakob, and H. von Löhneysen. T.P., I.T., and S.M. thank their home institutes for support from Institute of Physical Chemistry PAS, Kasprzaka 44/52, 01-224 Warsaw, Poland, A. V. Shubnikov Institute of Crystallography, RAS, 117333, Leninskii pr. 59, Moscow, Russia, and National Technical University "KhPI," Frunze Street 21, 61002 Kharkov, Ukraine, respectively.

*Corresponding author; felser@uni-mainz.de
†Corresponding author; m.jansen@fkf.mpg.de

[1] Y. A. Freiman and H. J. Jodl, Phys. Rep. **401**, 1 (2004).
[2] R. J. Meier and R. B. Helmholdt, Phys. Rev. B **29**, 1387 (1984).
[3] I. N. Goncharenko, O. L. Makarova, and L. Ulivi, Phys. Rev. Lett. **93**, 055502 (2004).
[4] Y. Akahama, H. Kawamura, D. Hausermann, M. Hanfland, and O. Shimomura, Phys. Rev. Lett. **74**, 4690 (1995).
[5] K. Shimizu, K. Suhara, M. Ikumo, M. I. Eremets, and K. Amaya, Nature (London) **393**, 767 (1998).
[6] M. Labhart, D. Raoux, W. Känzig, and M. A. Bösch, Phys. Rev. B **20**, 53 (1979).
[7] W. Hesse, M. Jansen, and W. Schnick, Prog. Solid State Chem. **19**, 47 (1989).
[8] M. Jansen and N. Korber, Z. Anorg. Allg. Chem. **598**, 163 (1991).
[9] A. Helms and W. Klemm, Z. Anorg. Allg. Chem. **242**, 33 (1939).
[10] A. Helms and W. Klemm, Z. Anorg. Allg. Chem. **241**, 97 (1939).
[11] A. Helms and W. Klemm, Z. Anorg. Allg. Chem. **242**, 201 (1939).
[12] S. Kuroiwa, Y. Saura, J. Akimitsu, M. Hiraishi, M. Miyazaki, K. H. Satoh, S. Takeshita, and R. Kadono, Phys. Rev. Lett. **100**, 097002 (2008).
[13] M. Jansen, R. Hagenmayer, and N. Korber, C.R. Acad. Sci., Ser. IIc: Chim **2**, 591 (1999).
[14] J. J. Attema, G. A. de Wijs, G. R. Blake, and R. A. de Groot, J. Am. Chem. Soc. **127**, 16325 (2005).
[15] J. Winterlik, G. H. Fecher, and C. Felser, J. Am. Chem. Soc. **129**, 6990 (2007).
[16] J. Winterlik, G. H. Fecher, C. A. Jenkins, C. Felser, C. Mühle, K. Doll, M. Jansen, L. M. Sandratskii, and J. Kübler, Phys. Rev. Lett. **102**, 016401 (2009).
[17] I. S. Elfimov, A. Rusydi, S. I. Csiszar, Z. Hu, H. H. Hsieh, H.-J. Lin, C. T. Chen, R. Liang, and G. A. Sawatzky, Phys. Rev. Lett. **98**, 137202 (2007).
[18] Y.-W. Son, M. L. Cohen, and S. G. Louie, Nature (London) **444**, 347 (2006).
[19] T. Bremm and M. Jansen, Z. Anorg. Allg. Chem. **610**, 64 (1992).
[20] H. Seyeda and M. Jansen, J. Chem. Soc. Dalton Trans. **1998**, 875.
[21] L. Hackspill, Helv. Chim. Acta **11**, 1003 (1928).
[22] G. Brauer, *Handbuch der Präparativen Anorganischen Chemie* (Enke-Verlag Stuttgart, Germany, 1978), Vol. 2.
[23] H. H. Eysel and S. Thym, Z. Anorg. Allg. Chem. **411**, 97 (1975).
[24] J. B. Bates, M. H. Brooker, and G. E. Boyd, Chem. Phys. Lett. **16**, 391 (1972).
[25] M. Rosenfeld, M. Ziegler, and W. Känzig, Helv. Phys. Acta **51**, 298 (1978).
[26] J. Schmalian and P. G. Wolynes, Phys. Rev. Lett. **85**, 836 (2000).